SCIENCE CHINA
Chemistry

• ARTICLES •
• SPECIAL TOPIC • New Researches of State Key Laboratories in Analytical Chemistry

July 2016 Vol.59 No.7: 802–808
doi: 10.1007/s11426-016-5575-2

A pH-responsive activatable aptamer probe for targeted cancer imaging based on i-motif-driven conformation alteration

Lv'an Yan[1,3,4], Hui Shi[1,3,4], Dinggeng He[1,3,4], Xiaoxiao He[1,2,4*], Kemin Wang[1,2,3,4*] & Fengzhou Xu[1,3,4]

[1]*State Key Laboratory of Chemo/Biosensing and Chemometrics; Hunan University, Changsha 410082, China*
[2]*College of Biology, Hunan University, Changsha 410082, China*
[3]*College of Chemistry and Chemical Engineering, Hunan University, Changsha 410082, China*
[4]*Key Laboratory for Bio-Nanotechnology and Molecular Engineering of Hunan Province; Hunan University, Changsha 410082, China*

Received September 26, 2015; accepted November 9, 2015; published online March 29, 2016

We present here a pH-responsive activatable aptamer probe for targeted cancer imaging based on i-motif-driven conformation alteration. This pH-responsive activatable aptamer probe is composed of two single-stranded DNA. One was used for target recognition, containing a central, target specific aptamer sequence at the 3′-end and an extension sequence at the 5′-end with 5-carboxytetramethylrhodamine (TAMRA) label (denoted as strand **A**). The other (strand **I**), being competent to work on the formation of i-motif structure, contained four stretches of the cytosine (C) rich domain and was labeled with a Black Hole Quencher 2 (BHQ2) at the 3′-end. At neutral or slightly alkaline pH, strand **I** was hybridized to the extension sequence of strand **A** to form a double-stranded DNA probe, termed i-motif-based activatable aptamer probe (I-AAP). Because of proximity-induced energy transfer, the I-AAP was in a "signal off" state. The slightly acidic pH enforced the strand **I** to form an intramolecular i-motif and then initiated the dehybridization of I-AAP, leading to fluorescence readout in the target recognition. As a demonstration, AS1411 aptamer was used for MCF-7 cells imaging. It was displayed that the I-AAP could be carried out for target cancer cells imaging after being activated in slightly acidic environment. The applicability of I-AAP for tumor tissues imaging has been also investigated by using the isolated MCF-7 tumor tissues. These results implied the I-AAP strategy is promising as a novel approach for cancer imaging.

aptamer, pH-responsive, activatable probe, cancer cell imaging, i-motif, tissue imaging

Citation: Yan LA, Shi H, He DG, He XX, Wang KM, Xu FZ. A pH-responsive activatable aptamer probe for targeted cancer imaging base on i-motif-driven conformation alteration. *Sci China Chem*, 2016, 59: 802−808, doi: 10.1007/s11426-016-5575-2

1 Introduction

Molecular targeting imaging of cancer is of great significance not only for early diagnosis of cancer but also for investigation of cancer metastasis [1,2]. Molecular probes are one of the key factors for successful cancer imaging. Compared with molecular probes currently available for cancer imaging, such as antibodies and enzymes, aptamers are emerging as promising candidates because of their high specificity, low molecular weight, lack of immunogenicity, easy and reproducible production, versatility in application, and easy manipulation [3,4]. With the development of systematic evolution of ligands by exponential enrichment for the selection of a panel of target cancer cell-specific aptamers, more and more aptamers against cancer cells have been selected and used as powerful targeting ligands for cancer imaging by using various signal reporters, including

*Corresponding authors (email: xiaoxiaohe@hnu.edu.cn; kmwang@hnu.edu.cn)

radioactive, magnetic, and fluorescent agents [5–7]. For example, Hicke *et al.* [5] labeled TTA1, an aptamer to the extracellular matrix protein tenascin-C in fluorescent and radiolabeled forms. The *in vivo* administration, uptake and tumor distribution of Rhodamine Red-X-labeled aptamer was studied by fluorescence microscopy. Simultaneously, images of the glioblastoma (U251) and breast cancer (MDA-MB-435) tumor xenografts were obtained by planar scintigraphy by using the ^{99m}Tc-labeled TTA1. Yu *et al.* [6] reported prostate-specific membrane antigen (PSMA) aptamer-conjugated thermally cross-linked superparamagnetic iron oxide nanoparticles (TCL-SPION) for prostate tumor detection *in vivo* by magnetic resonance imaging (MRI). Zhang *et al.* [7] reported a facile one-pot hydrothermal route to directly functionalize aptamer specific for mucin 1 with Zn-doped CdTe quantum dots (QDs) and used the as-prepared aptamer-QDs for tumor-targeted imaging *in vitro* and *in vivo*. In these reported aptamer probes based cancer imaging, it is not difficult to find that the aptamer probes for cancer imaging has primarily relied on the "always-on" design strategy. Through this design strategy, the aptamer probes for target cancer could be easily conjugated with signal reporters. However, the "always-on" aptamer probes require a long diagnosis time and often display lower imaging contrast owing to the high background originating from constant signals in nontarget tissues and blood [8].

To overcome the shortcoming of "always-on" aptamer probes for cancer imaging, our group firstly reported an activatable aptamer probe (AAP) for target cancer imaging, which was based on cell membrane protein-triggered conformation alteration [8]. The AAP is hairpin structured with a fluorophore and a quencher covalently attached at either terminus. Upon binding to target cancer cells, the AAP underwent a conformational alteration and displayed fluorescence. By compared with "always-on" aptamer probes, the AAP displayed substantially enhanced contrast and shortened diagnosis time. Subsequently, our group [9] also proposed another AAP strategy for cancer cells detection by using fluorophore-labeled aptamer/single-walled carbon nanotube (F-apt/SWNT) composites. "Signal on" AAP can also be designed by use of aptamer-modified gold nanoparticles (NPs) or magnetic NPs. For example, Tan *et al.* [10] utilized gold nanoparticles aggregation-induced signal enhancement to design AAP and develop a colorimetric assay for the direct detection of diseased cells. In addition to these mechanisms, tumor microenvironment signals, such as the acidic environment of tumor, can also be used to design AAP for targeted cancer imaging. To date, there is no relevant report.

The i-motif is a four-stranded DNA structure that can be formed from sequences containing stretches of cytosine (C) residues at slightly acidic pH. In this structure, two parallel duplexes maintained by hemi-protonated $C\cdot C^+$ base pairs are intercalated with each other in an antiparallel orientation [11,12]. At basic pH, the closed four-stranded structure can unfold to a single-stranded form. Taking advantage of the conformation alteration of i-motif at different pH, many i-motif based nanodevices have been designed and applied in the fields of pH change sensing and pH responsive controlled release [13–16]. By integrating the i-motif motor within other functional DNA structures, some DNA nanodevices with new functions such as i-motif-programmed DNA nanocircles [17], DNA nanosprings [18], and molecular logic gates [19,20] have also been reported. Moreover, it has been demonstrated that some nanodevices based on i-motif structures could work in living cells and *in vivo* [21–23].

Herein, we reported a pH-responsive activatable aptamer probe for targeted cancer imaging based on i-motif-driven conformation alteration. As illustrated in Figure 1, this activatable aptamer probe comprises two single-stranded DNA. One is a 27 mer single-stranded oligonucleotide **I** containing four stretches of the cytosine (C) rich domain. The strand **I** was labeled with a Black Hole Quencher 2 (BHQ2) at the 3′-end. The other is a 35 mer DNA strand **A**, which is composed of a central, target specific aptamer sequence at the 3′-end (in green) and an extension sequence at the 5′-end (in red). The extension sequence of strand **A** is partially complementary to the strand **I**. A fluorophore (TAMRA) was labeled at the 5′-end of strand **A**. At neutral or slightly alkaline pH, strand **I** is hybridized to the extension sequence of strand **A** to form a double-stranded DNA probe, termed i-motif-based activatable aptamer probe (I-AAP). The TAMRA at the 5′-end of strand **A** is kept in close proximity to the BHQ2 at the 3′-end of strand **I**. The I-AAP probe is then in a "signal off" state. However, in slightly acidic pH conditions, the C-rich domain of strand **I** can fold to an intramolecular i-motif through hemi-protonated cytosine-cytosine ($C\cdot C^+$) base pair formation, leading to the dehybridization of the duplex and the greater distance of fluorophore from the quencher. Thereupon, the fluorescence signal of strand **A** was activated, and the activated strand **A** carried out targeted imaging for the presence of target cancer cells. To demonstrate this principle, the imaging of MCF-7 cells was performed by using specific aptamer, AS1411.

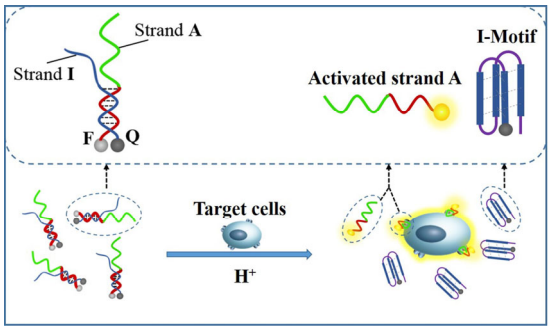

Figure 1 Schematic representation of the novel activatable aptamer probe strategy for target cancer cells imaging based on i-motif-driven conformation alteration (color online).

2 Experimental

2.1 Reagents and materials

All the DNA probes reported in this article were synthesized and purified (HPLC) by Sangon Biotechnology Co. Ltd. (China). Sequences of the DNA probes are listed in Table 1. Other chemical reagents used in this work were of the highest grade without further purification. The solutions of phosphate buffer (PB, 100 mmol/L) at the required pH were prepared using a mixture of NaH_2PO_4 and Na_2HPO_4, then adjusted slightly with HCl and NaOH. Deionized water was obtained from an in-house Barnstead Nanopure Infinity^{TM} ultrapure water system (Barnstead/Thermo-lyne Corp., USA).

MCF-7 cells line (human breast cancer cell) and SMMC-7721 cells line (human hepatocellular carcinoma cells) were purchased form the Shanghai Institute of Cell Biology of the Chinese Academy of Sciences. Cells were cultured at 37 °C in a humidified incubator containing 5% (*w*/*v*) CO_2. The culture medium is RPMI 1640 medium supplemented with 15% fetal bovine serum (FBS) and 100 IU/mL penicillin-streptomycin.

2.2 General methods

Fluorescence spectra were recorded on a Hitachi F-7000 FL Spectrophotometer (Japan) in PB buffer equipped with a Peltier temperature control accessory. Emission spectra were measured from 560 to 700 nm at 4 °C while exciting at 550 nm. The excitation and emission slits were both set at 5 nm.

UV-Vis absorption spectra were acquired on a Thermo Evolution 500 UV-visible Spectrophotometer (USA) equipped with a Peltier temperature control accessory. Absorption spectra were collected in the 220–320 nm range with a data interval of 0.2 nm and processed using OriginLab software. Melting curves of samples were measured at 295 nm from 4 to 40 °C.

Circular dichroism (CD) spectra were acquired on a Bio-Logic MOS-500 CD spectrophotometer (France) equipped with a Peltier temperature control accessory. CD spectra were recorded from 220 to 320 nm at 4 °C. The scanning processes were carried out according to previous literature [24].

Table 1 Names and sequences of all the DNA probes used in this work [a)]

DNA	Sequence (5′-3′)
AS1411	TAMRA-GGT GGT GGT GGT TGT GGT GGT GGT GG
Strand **A**	TAMRA-ATT GCA GGG TTA GGT GGT GGT GGT TGT GGT GGT GGT GG
Strand **A**′	TAMRA-ATT GCA GGG TTA GG N_{24}
Strand **I**	CCC TAA CCC TAA CCC TAA CCC TGC AAT-BHQ2
Strand **I**′	N_{13} CC TAA CCC TGC AAT-BHQ2

a) In all the sequences, the underlined bases represent in hybridization region and the N represents random base.

2.3 Construction of probes

An aptamer AS1411, a biologically active G-rich oligonucleotide, was used as a model system to demonstrate the feasibility of the I-AAP strategy for cancer imaging. It shows specific binding to nucleolin, a multifunctional protein that is highly expressed in a number of different cancer cells, both intracellularly and on the cell surface [25]. The strand **A** consisted of the AS1411 sequence at the 3′-end, an extension sequence and a fluorophore (TAMRA) covalently attached at the 5′-end. The strand **I** containing four stretches of the cytosine (C) rich domain and a quencher (BHQ2) covalently attached at the 3′-end. At neutral or slightly alkaline pH, strand **I** was hybridized to strand **A** with partially complementary to form I-AAP. Control probe **1** for the I-AAP consisted of the strand **A** and strand **I**′, the part of C-rich sequence in strand **I** was changed to a 13 mer random sequence, causing it to lose the ability to form i-motif. Analogously, control probe **2** for the I-AAP was constructed by the strand **A**′, the part of AS1411 sequence in strand **A** was changed to a 24 mer random sequence, hybridized with strand **I** such that it showed little affinity to target cancer cells. Hybridization process of all probes was carried out by mixing the corresponding DNA strands (1:1) with high concentration (100 μmol/L), and heated to 80 °C in water bath and then slowly cooled to 4 °C. The cooled DNA probes mixture was then stored in the dark on ice to allow hybridization. Before using, the hybridized probes were diluted to a certain concentration using a certain pH buffer or physiological saline.

2.4 Cells imaging

Cells were seeded on 35-mm glass bottom dish (MatTek, MA). After growing for one day in FBS, the cultured cells were then washed with 1 mL PB. The I-AAP was incubated with target MCF-7 cells or control SMCC-7721 cells in 500 μL PB on ice for 15 min at pH 7.0 and 6.5, respectively. All of the incubation was performed in the dark. Control probe **1** and control probe **2** were tested in a same manner in PB at pH 6.5. Then the samples were immediately determined with Olympus FV500 laser scanning confocal microscope (Japan). The probes concentration was fixed at 1 μmol/L. He Ne laser (543 nm) and a 560–610 nm bandpass filter were selected as the excitation light and the emission filter respectively.

2.5 *ex vivo* tumor tissues imaging

Male athymic BALB/c mice were purchased from the

Shanghai SLAC Laboratory Animal Co., Ltd. (China). Tumor-bearing animals were prepared through a subcutaneous injection of 5×10^6 *in vitro*-propagated MCF-7 cells into the backside of nude mice. The injected MCF-7 cells were then allowed to grow in the backside to form tumors with 1–2 cm in diameter. Before dissection, the tumor-bearing nude mice were anesthetized with both tranquilizer and anesthetic. Once the mice were anesthetized motionlessly, they will be killed by cervical dislocation. The tumor tissues and leg muscles, as negative control tissue, were isolated from the mice and washed for two times with physiological saline. After moving the isolated tissues onto the ice for 10 min, a 50 μL volume of physiological saline containing 0.25 nmol of I-AAP probes was directly injected into the isolated tumor tissues and leg muscles, respectively. The same dose of control probe **1** as a negative control probe was directly injected into the isolated tumor tissues. The probes were incubated with the isolated tissues on ice for 15 min in the dark. Next, fluorescence images of the probes treated isolated tissues were taken immediately by an IVIS Lumina II *in vivo* imaging system (Caliper Life-Sicence, USA). A 500–550 nm bandpass filter and a 575–650 nm bandpass filter were selected as the excitation filter and the emission filter respectively. In addition, It is notable that all animal operations were in accord with institutional animal use and care regulations, according to protocol No. SYXK (Xiang) 2008-0001, approved by the Laboratory Animal Center of Hunan (China).

3 Results and discussion

3.1 i-motif structure formation of strand I at slightly acidic pH

In this work, the strand **I** containing the human telomeric sequence (HT, $[C_3TA_2]_3C_3$) was served as pH response unit. To prove the conformational change of strand **I** upon pH change, we employed CD spectroscopies to characterize the strand **I** can form well-defined i-motif structure under slightly acidic pH at 4 °C. The different of CD spectra of strand **I** at several pH values (pH 7.4, 7.0, 6.5, and 6.0) are shown in Figure 2(a). As the pH decreased from 7.4 to 6.0, the positive band near 274 nm and the negative band near 244 nm, which are due to polynucleotide helicity and base stacking of unstructured ssDNA, are red-shifted to 287 and 256 nm with the increase of the ellipticity, respectively. These two distinct peaks near 287 and 256 nm are the characteristic spectrum of i-motif structures as reported previously [26]. These CD results demonstrated that the pH-induced conformational change of strand **I** went from the random coil to i-motif structure. This property was the foundation of i-motif-based nanodevices [27]. It is worth paying attention that the i-motif structure is unstable under the high temperature. The melting temperature (T_m) of

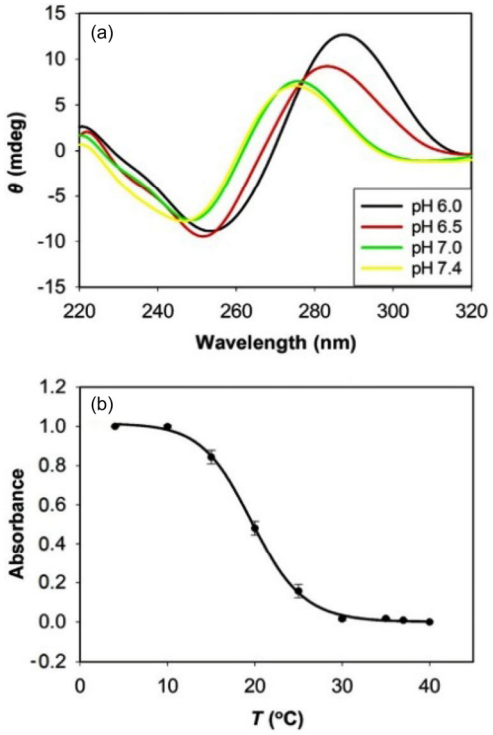

Figure 2 (a) The CD spectra of strand **I** recorded at different pH at 4 °C in 100 mmol/L PB; (b) UV melting curve of strand **I** at 295 nm at pH 6.5 buffer (color online).

strand **I** at pH 6.5 was obtained by plotting the normalized UV absorption value at 295 nm versus temperature (Figure 2(b)), the T_m was determined to be 19 °C. This temperature is much lower than physiological temperature (37 °C), which suggests this probe is unsuitable *in vivo*.

3.2 Activation performance of I-AAP

The above CD results clearly showed that the free strand **I** could form i-motif structure at slightly acidic pH. We then examined whether the formation of i-motif could break duplex structure of I-AAP to realize signal activation under acidic conditions. Fluorescence spectra measurements were used to determine the activation performance of I-AAP at different pH. As shown in Figure 3(a), at 4 °C, both emission spectra of I-AAP at pH 7.4 and 7.0 showed almost no fluorescence intensity at 580 nm which indicated the I-AAP maintained its double-stranded DNA structure. In this state, fluorophore was kept in close proximity to the quencher, causing the fluorescence quenching. However, by adjusting the pH to 6.5 and 6.0, respectively, we could observe that the fluorescence intensities increased obviously. It was displayed that the fluorescence of TAMRA was almost independent in the range of pH 6.0–7.4 (Figure S1, Supporting Information online). The results suggested that the strand **I** in the I-AAP folded into the i-motif form when the pH value was decreased, causing the duplex of I-AAP to be dissociated with an increase in fluorescence due to the greater

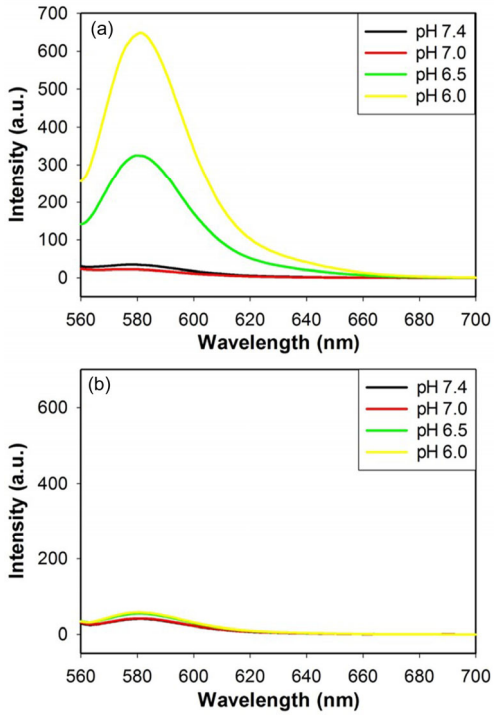

Figure 3 Fluorescence spectra of I-AAP (a) and control probe **1** (b) at 4 °C with different pH in PB (color online).

distance of TAMRA in strand **A** and BHQ2 in the strand **I**. For a control experiment, a strand **I**′ of the same length with strand **I** (which could not undergo a conformational transition with pH change) was used to hybridize with strand **A**. The formed probe was denoted as control probe **1**. It was demonstrated that the control probe **1** showed lower fluorescence intensities in all of the different solution, which indicated that the control probe **1** could not be activated at slightly acidic pH (Figure 3(b)). Therefore, the changes of the fluorescence intensities of the I-AAP with decreasing pH were closely related to the conformational change of i-motif sequence.

3.3 Target cells imaging by using I-AAP

After confirming the I-AAP could be activated under the slightly acidic pH, we then investigated the I-AAP probe for target cells imaging by using laser scanning confocal microscope experiments. MCF-7 cells line, a nucleolin highly expressed cells line, was chosen as target cancer cells, and SMCC-7721 cells line was served as negative control cells [25]. As described in the design, the strand **I** was competent to work on the formation of i-motif structure, while the strand **A** in the I-AAP was responsible for target recognition. Following the design, we firstly investigated the feasibility of the aptamer AS1411 contained strand **A** for target MCF-7 cells recognition. It was demonstrated that the aptamer AS1411 contained strand **A** could still specifically recognize target MCF-7 cells like that of the aptamer AS1411, as indicated by strong fluorescence in MCF-7 cells. While it could not recognize SMCC-7721 cells (Figure S2). Subsequently, the target cells imaging of I-AAP was tested. Two different pH conditions, including pH 7.4 and 6.5, have been selected. Two control probes were also used. One was control probe **1** in which the strand **I**′ could not form i-motif under the slightly acidic pH. The other was control probe **2** by changing the AS1411 sequence in strand **A** to random DNA sequence. The imaging analysis results are shown in Figure 4. From the imaging results, we could observe that the MCF-7 cells incubated with the I-AAP at pH 6.5 displayed obvious fluorescence. However, no or very little fluorescence signal was observed for all of the control groups, including I-AAP incubated SMCC-7721 cells at pH 6.5, I-AAP incubated MCF-7 cells at pH 7.4, I-AAP incubated SMCC-7721 cells at pH 7.4, control probe **1** incubated MCF-7 cells at pH 6.5, control probe **1** incubated SMCC-7721 cells at pH 6.5, control probe **2** incubated MCF-7 cells at pH 6.5, and control probe **2** incubated SMCC-7721 cells at pH 6.5. Because I-AAP is a "signal off" state at slightly alkaline pH, the target MCF-7 cells have not been dyed with I-AAP at physiological pH 7.4 (Figure 4(a)). When the solution pH was changed to 6.5, the fluorescence signal of strand **A** was bright around the MCF-7 cells (Figure 4(c)). Simultaneously, The fluorescence signal of control probe **1** could not be activated at pH 6.5 because the strand **I**′ could not be released through configuration transformation. However, control probe **2** could be activated

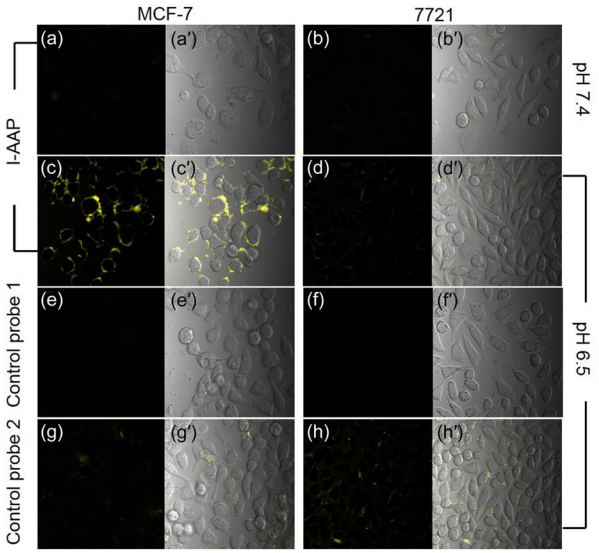

Figure 4 The i-motif-driven conformation alteration based I-AAP for target cell imaging. (a–h) The fluorescence images. (a) I-AAP incubated MCF-7 cells at pH 7.4; (b) I-AAP probe incubated SMCC-7721 cells at pH 7.4; (c) I-AAP incubated MCF-7 cells at pH 6.5; (d) I-AAP incubated SMCC-7721 cells at pH 6.5; (e) control probe **1** incubated MCF-7 cells at pH 6.5; (f) control probe **1** incubated SMCC-7721 cells at pH 6.5; (g) control probe **2** incubated MCF-7 cells at pH 6.5; (h) control probe **2** incubated SMCC-7721 cells at pH 6.5. The images of (a′–h′) were corresponding merged images (color online).

at pH 6.5 theoretically, but the strand **A′** could not specifically recognize the target cells, so it was observed that both of them showed unmarked fluorescence label of MCF-7 cells (Figure 4(e, g)). These results suggested that the I-AAP could be activated by slightly acidic environment due to the configuration transformation of i-motif, and carried out for target cancer cells imaging. By compared with the "always-on" AS1411 aptamer probe for the target cells imaging, the I-AAP showed lower background fluorescence (Figure S3).

3.4 Tumor tissues imaging by using I-AAP

Tumor acidic microenvironment is considered as a cancer hallmark, which is ubiquitous in solid tumors even regardless of cancer type [28]. We just have demonstrated that the I-AAP cloud recognize and labeled the target cancer cells in the slightly acidic pH solution. We further investigated the capability of I-AAP activation in target tumor tissues. Figure 5(a) (middle) displays fluorescence images of the isolated MCF-7 tumor after direct injection of 0.25 nmol I-AAP at 30-min postinjection time. It was clearly observed that the fluorescence signal of I-AAP was activated. At the same time, two control groups were performed. The one was that the control probe **1** was directly injected into the isolated MCF-7 tumor, as shown in Figure 5(a) (left). There was almost no fluorescence detected because the control probe **1** could not respond to slightly acidic pH. The other one was the isolated thigh muscle injected into with I-AAP directly, as shown in Figure 5(a) (right). The pH of muscle tissue is about 7.4, so I-AAP kept in "signal off" state. These results suggested that the fluorescence signal of I-AAP could be activated specifically by tumor's slightly acidic environment, and the I-AAP strategy is promising as a novel approach for *in vivo* cancer imaging.

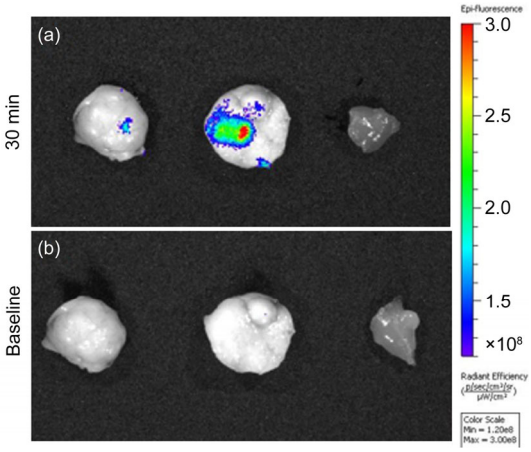

Figure 5 The i-motif-driven conformation alteration based I-AAP for tumor tissues imaging. (a) The fluorescence images of the isolated tumor tissue injected with control probe **1** (left), the isolated tumor tissue injected with I-AAP (middle), and the isolated thigh muscle injected with I-AAP (right); (b) baseline of corresponding tissues (color online).

4 Conclusions

By combining the tumor acidic microenvironment signal and i-motif-driven conformation alteration, we have developed an activatable aptamer probe strategy for targeted cancer imaging. The double strand i-motif-based activatable aptamer probe, containing strand **A** for target recognition and strand **I** for i-motif formation (named as I-AAP), underwent dehybridization in a slightly acidic pH environment due to the formation of intramolecular i-motif. Thus the activated fluorescence was readout in the target binding. As proof of concept, the AS1411 aptamer against nucleolin was used. It was found that the I-AAP indeed could be activated in the slightly acidic pH solution. Subsequent *in vitro* assays confirmed that the I-AAP could specifically image the target MCF-7 cells in a slightly acidic environment. Tumor tissues imaging was also preliminarily tested. The design of the probe is simple and the response is rapid. By substituting the aptamer sequence to suit to other targets, this strategy has the potential to be developed to a universal method for a wide variety of cancer imaging. Unfortunately, the problem is that the i-motif structure formed by strand **I** in this work is unstable under the high temperature. For the *in vivo* application in future, we should introduce i-motif structure with high value of T_m for designing the activatable aptamer probe.

Acknowledgments This work was supported by the Key Project of National Natural Science Foundation of China (21175039, 21322509, 21305035, 21190044, 21221003, 21305038, 2015JJ3044).

Conflict of interest The authors declare that they have no conflict of interest.

Supporting information The supporting information is available online at chem.scichina.com and link.springer.com/journal/11426. The supporting materials are published as submitted, without typesetting or editing. The responsibility for scientific accuracy and content remains entirely with the authors.

1 Becker A, Hessenius C, Licha K, Ebert B, Sukowski U, Semmler W, Wiedenmann B, Grötzinger C. *Nat Biotechnol*, 2001, 19: 327–331
2 Cerchia L, Franciscis VD. *Trends Biotechnol*, 2010, 28: 517–525
3 Tan WH, Michael JD, Jiang JH. *Chem Rev*, 2013, 113: 2842–2862
4 Schmidt KS, Borkowski SJ, Stephens AW, Bald R, Hecht M, Friebe M, Dinkelborg L, Erdmann VA. *Nucleic Acids Res*, 2004, 32: 5757–5765
5 Hicke BJ, Stephens AW, Gould T, Chang YF, Lynott CK, Heil J, Borkowski S, Hilger CS, Cook G, Warren S, Schmidt PG. *J Nucl Med*, 2006, 47: 668–678
6 Yu MK, Kim D, Lee IH, So JS, Jeong YY, Jon S. *Small*, 2011, 7: 2241–2249
7 Zhang CL, Ji XH, Zhang Y, Zhou GH, Ke XL, Wang HZ, Tinnefeld P, He ZK. *Anal Chem*, 2013, 85: 5843–5849
8 Shi H, He XX, Wang KM, Wu X, Ye XS, Guo QP, Tan WH, Qing ZH, Yang XH, Zhou B. *Proc Natl Acad Sci USA*, 2011, 108: 3900–3905
9 Yan LA, Shi H, He XX, Wang KM, Tang JL, Chen M, Ye XS, Xu FZ, Lei YL. *Anal Chem*, 2014, 86: 9271–9277
10 Medley CD, Smith JE, Tang ZW, Wu YR, Bamrungsap S, Tan WH.

Anal Chem, 2008, 80: 1067–1072
11 Leroy JL. *Nucleic Acids Res*, 2009, 37: 4127–4134
12 Song GT, Ren JS. *Chem Commun*, 2010, 46: 7283–7294
13 Chen LF, Di JC, Cao CY, Zhao Y, Ma Y, Luo J, Wen YQ, Song WG, Song YL, Jiang L. *Chem Commun*, 2011, 47: 2850–2852
14 Li W, Wang JS, Ren JS, Qu XG. *Angew Chem Int Ed*, 2013, 52: 6726–6730
15 Nesterova IV, Nesterov EE. *J Am Chem Soc*, 2014, 136: 8843–8846
16 Dembska A, Juskowiak B. *Spectroc Acta Pt A: Molec Biomolec Spectr*, 2015, 150: 928–933
17 Li T, Famulok M. *J Am Chem Soc,* 2013, 136: 1593–1599
18 Wang C, Huang Z, Lin Y, Ren J, Qu X. *Adv Mater*, 2010, 22: 2792–2798
19 Li J, Huang YQ, Qin WS, Liu XF, Huang W. *Polym Chem*, 2011, 2: 1341–1346
20 Pu F, Wang CY, Hu D, Huang ZZ, Ren JS, Wang S, Qu XG. *Mol BioSyst*, 2010, 6: 1928–1932
21 Huang J, Ying L, Yang XH, Yang YJ, Quan K, Wang H, Xie NL, Ou M, Zhou QF, Wang KM. *Anal Chem*, 2015, 87: 8724–8731
22 Surana S, Bhat JM, Koushika SP, Krishnan Y. *Nat Commun*, 2011, 2: 340
23 Modi S, Nizak C, Surana S, Halder S, Krishnan Y. *Nat Nanotech*, 2013, 8: 459–467
24 Zhou J, Wei CY, Jia GQ, Wang XL, Feng ZC, Li C. *Mol BioSyst*, 2010, 6: 580–586
25 Bates PJ, Laber DA, Miller DM, Thomas SD, Trent JO. *Exp Mol Pathol*, 2009, 86: 151–164
26 Choi J, Kim S, Tachikawa T, Fujitsuka M, Majima T. *J Am Chem Soc*, 2011, 133: 16146–16153
27 Dong YC, Yang ZQ, Liu DS. *Acc Chem Res*, 2014, 47: 1853–1860
28 Kato Y, Ozawa S, Miyamoto C, Maehata Y, Atsuko Suzuki A, Maeda T. *Cancer Cell Int*, 2013, 13: 89